Continuous Long-Range Thunderstorm Monitoring by a VLF Receiver Network. Part II: Cloud-to-Ground and Intra-Cloud Detection Efficiency

Carlos A. Morales*
Department of Civil and Environmental Engineering
University of Connecticut, Storrs, CT

James A. Weinman
Microwave Sensors Branch
NASA Goddard Space Flight Center, Greenbelt, MD

Emmanouil N. Anagnostou
Department of Civil and Environmental Engineering
University of Connecticut, Storrs, CT

Steve Goodman
Global Hydrology Center
NASA Marshall Space Flight Center, Alabama

Earle Williams
Department of Civil and Environmental Engineering
MIT, Boston, MA

*Current Affiliation: Atmospheric Sciences Department,
Colorado State University, Fort Collins, CO

In preparation to be submitted to *Journal of Atmospheric and Oceanic Technology*

July 2002

ABSTRACT

The cloud-to-ground (CG) and intra-cloud (IC) lightning detection efficiency of an experimental long-range Very Low Frequency (VLF) lightning network named Sferics Timing and Ranging Network (STARNET) is examined using as reference the more definitive measurements from the National Lightning Detection Network (NLDN) and the Lightning Detection and Ranging (LDAR) systems. Furthermore, bulk IC:CG relative ratio statistics over the continental US are derived using LDAR, NLDN and STARNET measurements. The STARNET CG detection efficiency (DE) derived theoretically and experimentally using NLDN shows exponential range dependence that varies from 100%, within the network (East Coast of US), down to about 20% at distances over 4,000 km. Day and night DE differences are negligible. The STARNET's CG (IC) DE evaluated using LDAR data over a limited area in Florida-US is shown to vary from 57% (7%) to 70% (19%). During daytime (nighttime) period the CG and IC DE ranged from 68% (49%) to 78% (67%) and 4% (9%) to 9% (29%), respectively. The bulk IC:CG ratio values derived using STARNET and NLDN over the continental US showed a range of 0-4. In a finer scale resolution, over Florida-US and for selected storm cases, the 0-4 IC:CG range is shown to account for ~50% of the observed values. At this scale LDAR estimates show IC:CG ratios ranging up to 15.

1. Introduction

Lightning measurements have been extensively used by power companies, meteorological offices, air chemistry, forestry services, commercial and military aviation, and by the scientific community in general. The application of such measurements depends on the type of lightning, e.g. Cloud-to-Ground, CG, and Intra-cloud, IC, as well as its location accuracy and detection efficiency (DE). Lightning emits electromagnetic radiation during its breakdown and ionization process and it is observed at Very Low Frequency (VLF), Low Frequency (LF), High Frequency (HF) and at Very High Frequency (VHF), e.g., Malan (1963) and Pierce (1977). The CG lightning is mainly observed at VLF and LF, while IC dominates the VHF band. This frequency dependence limits the range of lightning measurements associated with a single type of sensor. Additionally, the location accuracy and detection efficiency of a lightning measurement is affected by the propagation of electromagnetic radiation through the earth-ionosphere waveguide medium.

Location accuracy has been subject of several studies associated with lightning location (Krider et al., 1976; Lewis, 1960, Lee, 1986a,b; Cummins et al, 1998; Proctor, 1971; Koshak and Solakiewicz, 1996; Morales et al., this issue). At shorter distances most of the lightning networks that use varying methodologies have high location accuracy. The main problem with these methodologies is the distant lightning sources, beyond 1,000 km, where the propagation effect degrades the signal. Moreover, it diminishes the location accuracy and consequently the detection of weaker lightning strokes (Lee, 1989; Cramer and Cummins, 1999; and Morales et al., this issue).

The expected detection efficiency of any instrument can be evaluated in laboratory experiments or by determining the sensor response to its measurement. This is accomplished by knowing the properties of the data to be measured. The "true" IC and CG lightning distribution is still unknown, despite recent measurement systems that claim high detection efficiency for each type of lightning (Cummins et al., 1998 and Boccippio et al., 2000a, Mazur et al., 1997). Consequently, lightning detection efficiency (DE) evaluation of a system may be determined relatively to those high DE instruments that measure the same type of source.

STARNET is an experimental lightning network designed to measure sferics, radio noise produced by lightning in the VLF spectrum, over long ranges (up to a few thousand of kilometers). The system is described in Morales et al. (this issue) where it is shown to have relative location accuracy of 0-10 km on the East Coast of US, 50-60 km on the West Coast of the US, and below ~50 km over the North Atlantic ocean and western South America. These relative errors were retrieved by comparing STARNET measurements with the National Lightning Detection Network (NLDN) CG monitoring network, Cummins et al. (1998a), the Lightning Imaging Sensor (LIS), Christian et al. (1999), and through numerical simulation of expected error sources, Morales et al. (this issue).

This paper aims at characterizing the STARNET's DE of CG and IC lightning. The DE is studied through comparison with more established lightning systems such as the NLDN and the Lightning Detection and Ranging (LDAR) system in Florida-US, Lennon and Maier (1991). Consequently, the DE estimates are relative to the measurements obtained by those networks. The three networks operate in different frequency domains: STARNET is at VLF centered at 9.8 kHz; NLDN is a wideband LF/VLF (2-500 kHz); and LDAR a VHF at 66 MHz. Therefore, each system measures different parts of the radiation source emitted by a lightning strike. Thus, the

analysis presented herein is carefully made as each system may measure some lightning sources that are not observed by the other systems.

The NLDN system described by Cummins et al. (1998b) has a DE for CG flashes ranging from 80-90% over the continental US (Cummins et al., 1998a; Orville, 1991; and Idone et al., 1998). Cummins et al. (1998a) obtained those DE values through numerical simulation of the electric field that propagates to a radio receiver by assuming peak current distribution. Orville (1991) compared NLDN measurements with triggered lightning return strokes. Idone et al. (1998) compared lightning video records data in Albany-NY with those from NLDN during three consecutive summers. Those experiments were conducted over selected regions in the US that had optimal sensor configurations. The transferability of these results to other US regions is not straightforward and consequently the DE estimates derived from NLDN are subject to uncertainty. The LDAR system measures both IC and CG lightning sources and it is limited to a range of 100-200 km due to attenuation and line-of-sight propagation effects, Mazur et al. (1997) and Boccippio et al. (2001a). Boccippio et al. (2001b) computed a DE of 90% for measurements within 100 km from the central station and an exponential decay to 25% at around 200 km range.

The following sections of this paper describe a methodology for retrieving relative CG and IC detection efficiency, and its application to compute ratios of IC to CG (IC:CG) over the continental US to support the IC measurements in the STARNET system. Next section provides a short background on STARNET system. Sections 3 and 4 describe STARNET's CG and IC detection efficiency evaluation, respectively. Section 5 describes IC:CG ratio evaluation, and finally in Section 6 we offer our conclusions and discussion on unresolved issues.

2. STARNET background

STARNET uses the general concept developed by Lee (1986b) on an operational Arrival Time Difference (ATD) system, while applying the current Internet and GPS technology not available at the time in Lee's system. Detailed description of STARNET system is provided in Morales et al. (this issue), while herein we provide abstractly its main aspects. This current experimental system operates with five radio receivers in the VLF spectrum between 5 and 15 kHz centered at 9.8 kHz (i.e., sferics). The receivers are located in Greenwich, RI, Fairfax, VA, Huntsville, AL, Miami, FL and San Juan, PR, as illustrated in Figure 1. They measure the vertical electric field that is time-stamped and synchronized with a GPS clock with an accuracy of 1 μsec. These continuous measurements represent sferics waveforms that are packed in 13.1 millisecond time windows. The present configuration supports sampling of 70 sferics/second. Once the waveforms from each receiver are transmitted to the central station, a signal-processing algorithm computes the ATD values for all receiver pair combinations. These ATDs represent regions between two outstations that have the same time difference, that are approximately as hyperbolas in the earth's surface. Maximizing the time correlation between two receiver waveforms derives the estimation of an ATD. The intersection of the ATD hyperbolas defines a lightning position fix, Lee (1986a). Intrinsic signal processing random errors and bias due to propagation effects introduce uncertainty on the location accuracy of lightning derived by those sensors (Lee, 1986a, 1986b, 1989; and Morales et al., this issue). Morales et al. (this issue) have developed and studied location error correction schemes for STARNET. Nevertheless, an important issue of this long-range lightning-measuring network is its efficiency for detecting

both CG and IC lightning at various ranges. In the subsequently sections we investigate those issues.

3. CG Detection Efficiency

STARNET measures sferics at VLF region, where cloud-to-ground (CG) lightning dominates the emission of radiation source (Pierce, 1977). At VLF frequencies, where STARNET radio receivers operate, range and temporal effects can introduce significant variability to the relationship of their measurement to lightning. This is due to the changes in the attenuating medium, height of the ionosphere waveguide, and the propagation direction and location within the waveguide (Saxton, 1964, and Wait, 1970). The sferics electric field signal propagates through the earth-ionosphere waveguide until it reaches the radio receivers. During this propagation, the electromagnetic radiation emitted by a lightning discharge interacts with the bounded medium and interference occurs. This interference attenuates the electric field in addition to delaying or speeding its propagation, which introduces distortion in the electrical waveforms observed by the receivers.

The attenuation is dependent on the Earth's surface properties (due to differences in ground conductivity between land and water), changes in the ionosphere height during day and nighttime, and finally the propagation direction (e.g., east-west, west-east, south-north, and north-south). Attenuation coefficients have been retrieved experimentally for most of those scenarios and have been summarized by Chapman and Macario (1956). Challinor (1967) and Taylor (1960a) presented attenuation values of 2.4 dB/1000 km for daytime propagation. During nighttime, Chapman and Macario (1956) showed a value near 2 dB/1000 km. Taylor (1960b)

and Taylor and Lange (1958) on east-west and west-east sferics propagation found attenuation values ranging from 3.0-4.5 dB/1000 km over land and 2.5-3.6 dB/1000 km over sea surface.

Horner (1964), using a VLF wave propagation model, determined an empirical relationship to obtain the electric field strength as a function of the lightning source position and path attenuation for different frequencies and it is expressed as follow:

$$E = A\left[\frac{\exp\left\{-\frac{\alpha d}{8680}\right\}}{\sqrt{\sin\left(\frac{d}{R}\right)}}\right](Volts/m) \qquad (1)$$

where A is a constant in Volts/m, R is the earth's radius in km, and d is the distance from the lightning source to the receiver (in km), and finally α is the attenuation coefficient (in dB/Mm). At zero distances, namely over a receiver's location, the electric field strength is set equal to A.

Equation 1 is used herein to evaluate the normalized electric signal strength of the present STARNET configuration. The electric field strength of each receiver with location shown in Figure 1 is computed as follows. First, the geodesic distance (distance along a great circle path) between the lightning source and the receiver is evaluated. Second, the portions of land and ocean propagation, as well as propagation direction are determined. Third, the minimum electric field strength observed by all the receivers for a particular lightning source is selected. Finally, electric field values are normalized by the maximum value in the simulated data array and presented in percent. The above expression offers a simplistic computation of the expected DE. As already listed, most of the attenuation information that accounts for different propagation direction in the literature exists for daytime conditions. Therefore the normalized electric field

strength is computed only for daytime, but distinguished to different paths (i.e., land vs. sea surfaces) and propagation directions (i.e., West-East and East-West). Table 1 shows the attenuation coefficient values used for the different path and propagation direction cases.

To compare the above theoretical model with experimental CG DE estimates, shown in section 3.1, we computed the mean CG DE values over the continental US as a function of longitude zone. Figure 2a shows the daytime longitudinal variation of the normalized signal strength for the present configuration of STARNET derived from the above model applied to the continental US (black line). It is noted that at ranges up to approximately 4,000 km the signal strength is considerable (~20%). These simplistic results are combined with the experimental CG DE values discussed in the next section to derive a better characterization of the spatial distribution of STARNET's CG DE.

3.1 Experimental CG DE: STARNET vs. NLDN comparison

The CG measurements from NLDN are used herein as a benchmark over the US region for testing the STARNET's ability to measure CG. Cummins et al. (1998a) have shown that the NLDN has an efficiency of 80-90% in measuring CG lightning over the US. Boccippio et al. (2001c) have described a method for retrieving CG detection efficiency of the Optical Transient Detector (OTD) system onboard MICROLAB Low Earth Orbiting (LEO) satellite, Christian et al. (1996), over the US using NLDN. They defined the DE in a probabilistic way, where the intrinsic errors of the instruments and locating algorithm (such as location and timing errors) are taken jointly into consideration. We have deployed a similar scheme for evaluating the overall STARNET's CG detection efficiency with respect to NLDN lightning over the continental US.

The scheme consists of determining the number of STARNET sferics and NLDN flash matches ($N_{Sferics}$) that fall within a space (ε_{rmax}) and timing (ε_{tmax}) window and the total number of CG NLDN lightning observed (N_{NLDN}) within the above window. The DE is subsequently expressed as:

$$DE_{(Sferics/CG-NLDN)} = \frac{N_{Sferics}(\varepsilon_{r\max}, |\varepsilon_{t\max}|)}{N_{NLDN}} \qquad (2)$$

Flashes consist of several strokes in the same area with time duration that can last up to one second (NLDN definition presented by Cummins et al., 1998a). Subsequently, varying space and time windowing is used to obtain the maximum compromise for STARNET's CG flash detection efficiency (DE). Table 2 summarizes the total number of sferics/flash matches for different combinations of space and timing windows over the period December 1997 through February 1998 in the continental US. It is noted that for the above period there were 871,450 CG NLDN flashes (1,751,040 strokes) within the US, while the flashes with current peak between 0-10 kA have been filtered out in this data set due to expected contamination of IC (Cummins et al., 1998a; Wacker and Orville, 1999a and 1999b). It is apparent from Table 2 that smaller space-time constraints result in fewer matches. For this same period 1,095,928 sferics were observed over the continental US. The NLDN flash time duration interval used in clustering the strokes was not available. Thus, each matched NLDN flash was scaled by its stroke multiplicity. Consequently, the evaluation of CG-DE expressed in equation (2) uses sferics from STARNET and strokes from matched NLDN flashes multiplied by NLDN's DE (1/0.9).

The space and time dependence of the STARNET DE was analyzed by evaluating equation (2) over matches that fall in time intervals of 15 minutes and areas grouped in 2-degree longitude zones within the US. The 15 minutes DE values are subsequently averaged to hourly values and assigned to the local time (LT) of the particular longitudinal zone. Moreover, day, night, and twilight time zones are separated and mean values for each set are evaluated. Daytime is defined from 08:00 to 16:59 LT, nighttime from 20:00 to 04:59 LT, daytime twilight from 05:00 to 07:59 LT, and finally nighttime twilight from 17:00 to 19:59 LT.

Figures 2 and 3 show the day/night and twilight time mean CG detection efficiency of STARNET sferics for 100 msec timing and 50 km space window. The location accuracy presented by Morales et al. (this issue) and its combination with the results shown in Table 2 indicate that the 100 msec and 50 km time and space values should represent the best compromise on location errors and duration of a flash. Consequently, these values are selected in the analysis that follows. The scatter plots in Figures 2 and 3 show DE values above 100% over the East Coast. These anomalous DE values could indicate that: (1) NLDN CG DE is lower than it was computed by Cummins et al. (1998a) and Idone et al. (1998); (2) there is IC sferics inflation for the selected space and time window over that region; and (3) some observed sferics are not measured by NLDN since the two systems use different frequency ranges in their measurements. We lean towards the second issue since we expect some IC sferics measurements to occur due to the high detection efficiency at the East Coast where all five ground receivers are located. In the subsequent analyses these anomalous values were excluded from the regression fitting. At longitudes between 105-120W, the CG-DE efficiency falls off from the general exponential trend observed. Boccippio et al. (2001c) have also found higher ratios of IC:CG at that region, which indicates IC sferics inflation. Their analyses showed that this high IC:CG

ratio anomaly is associated with strong positive cloud-to-ground strokes and the presence of mesoscale convective systems (MCS). Later in section 5, the IC:CG ratios are evaluated and this effect becomes more evident.

The CG DE for day and night shows similar exponential decay with distance westward from the East Coast network. The main difference observed during this time interval is that there is a slightly faster decay during the daytime period and an indication of more IC inflation. This last effect is substantiated in Sections 4 and 5. The two twilight intervals show no difference and are quite similar to the daytime decay. The above analyses indicate that STARNET main location algorithm and its signal processing were able to account for the differences in the signal strength attenuation observed during daytime and nighttime.

The mean DE of CG flashes along the East Coast is near 100% and falls exponentially toward the West Coast. Following the exponential decay shown in the figure daytime and nighttime DE reaches 16% and 18% at the West Coast. Table 3 summarizes the relationships obtained for the CG flashes DE presented in Figures 2 and 3. It is apparent that the intercepts and slopes of all time intervals are almost the same except for the nighttime period. This may be an effect of the lower IC concentration during nighttime. In the next section, the IC detection is explored to understand the anomalous DE values presented herein.

The theoretical expected CG DE displayed in Figure 2a shows very good agreement with the experimentally retrieved, as illustrated by the least-square fit (blue line). These results encouraged the application of Horner's model adjusted with the experimental results to obtain the spatial distribution of CG-DE over other regions. Subsequently, the theoretical mean signal strength values (black line, Figure 2a) were normalized with respect to the least-square fit of the experimentally derived CG DE values for daytime as shown in Table 2. Figure 4 shows the

spatial distribution of the normalized theoretical CG DE values. Assuming that in the present comparisons, STARNET was able to measure sferics along the West Coast of US, it is reasonable to expect that the 20% DE isochrones delineate the main regions of STARNET coverage.

4. Intra-Cloud Detection Efficiency

This section describes inter-comparison of three lightning networks, i.e., LDAR, NLDN, and STARNET aiming at investigating the detection frequency of intra-cloud (IC) from STARNET (IC DE). The LDAR measurements were made available by the Global Hydrology Resource Center of MSFC/NASA in the form of files containing the 3D Cartesian coordinate locations of lightning sources and respective times (in microseconds). Those Cartesian coordinates are referred to a central LDAR station (located in Cape Canaveral, Florida) along a tangent parallel plane and correspond to east, north, and vertical (i.e., height) displacements from the origin (Poehler and Lennon, 1979). The measurements were converted from their Cartesian system to latitude and longitude locations over the earth's surface using a geodetic earth model, while altitude was corrected for the earth's curvature effect. Raw LDAR data were analyzed for quality control. The analysis indicated periodic observations at 60 Hz (calibration test pulse) as well as continuous measurements (associated with aircraft tracks) along the coast of Florida, which were independently verified (personal communication with Dr. Dennis Boccippio) and discussed in Boccippio et al. (2001a). Consequently, LDAR raw data were manually filtered to correct for those effects.

The following sub-sections are carried out to develop a methodology for computing the IC measurements on both STARNET and NLDN networks. Each lightning network measures different parts of lightning radiation and it provides its own data structure/format. As consequence, lightning flashes are adopted as the standard lightning definition for this comparison. Consequently, LDAR and STARNET lightning flashes are characterized. Upon this standardization, all three networks are brought together to seek IC and CG characterizations on flash polarity, peak current distribution, and altitude.

4.1 Characterization of lightning flashes

Quality controlled LDAR data were stored in 15-minute interval files to be consistent with the NLDN and STARNET data sets. In each 15-minute interval file LDAR sources were grouped into clusters representing individual storm systems. LDAR sources were subsequently sorted by time of occurrence to be grouped into flashes according to the following condition (Boccippio et al., 2001a): A flash is composed of LDAR sources occurring within a 2 second time window and 50 km spatial extent (Boccippio et al. 2001a,b applied 65 km extension). The latitude, longitude, and altitude positions of the flash were used to determine the mean value of the clustered LDAR sources. For reference the time duration and the minimum observed height of a flash were stored in the processed database. Figure 5a shows the frequency distribution of the number of sources per flash identified based on the above criterion in the period of December 1997 through February 1998 for storms within 100km from the LDAR central station. These results are similar to the distribution presented by Boccippio et al. (2001a). The time interval

distribution for a flash, not shown here, is mainly concentrated below one second, which is consistent with Boccippio et al. (2001a) findings.

The STARNET measurements were also clustered and ordered by time of occurrence to compute flashes. In this conversion the time-space window was chosen to be 500 milliseconds (separation between two sferics candidates) and 50 km respectively, which is consistent with NLDN's procedures for converting strokes to flashes, Cummins et al. (1998a). It is noted that the time differences of sferics for the flashes derived in this study (not shown here) did not exceed 100 milliseconds. The frequency distribution of the number of sferics per flash is presented in Figure 5b. In the same plot it is shown the distribution of NLDN strokes per flash. Both NLDN and STARNET networks have a maximum peak of 1 sferics (or stroke) per flash and show very similar statistical distributions. This result verifies our initial assumption that the number of sferics events per flash is equivalent to the number of NLDN strokes per flash.

Coincident (in time and space) matches of observed flashes by LDAR, STARNET, and NLDN networks were identified for each cluster of the 15-minute storm files. The matching consists of finding a flash of one system occurring in the others within a certain time window. Since the LDAR system originally measures a much larger number of sources (see Figure 5a) a time window of $\pm$ 250 milliseconds was set for searching coincident measurements for NLDN and STARNET. The above time interval was chosen because according to Figure 6a (to be discussed later) the time lag distribution tails off at about that value. For matching STARNET and NLDN flashes a 100 milliseconds time window was applied. No distance constraint was established since matching was applied within the same selected storm cluster. The LDAR system has an expected detection efficiency greater than 90% for measurements within 100km from the central station (Boccippio et al. 2001a,b), while it drops to 25% at ranges further than

200 km. Consequently, this matching analysis included only storm clusters from ranges less than 100km range. The storms were selected manually to guarantee the cluster matching and elimination of intense thunderstorms that have very high number of flash rates, which might introduce erroneous LDAR flash classification.

The above procedure led to 301 storm cluster files with a total of 2,132 LDAR-STARNET, 1,707 LDAR-NLDN and 2,961 NLDN-STARNET matched flashes. Figures 6a, 6b, and 6c show the time lag distribution (in milliseconds) for the LDAR-STARNET, LDAR-NLDN, and NLDN-STARNET matches, while Table 4 shows the percentage of matched flashes and the total number of flashes observed by each network assuming the above time window constraint.

A mean time lag of -19.39 and -21.89 milliseconds between LDAR and respective STARNET and NLDN matched flashes shows the delay that both systems have in measuring a same event observed by LDAR. This time delay suggests that NLDN and STARNET system measurements missed the earlier breakdown lightning stages measured by the LDAR system. The wide distribution of time lags presented in Figures 6a and 6b can be attributed to the 2-seconds time window used to derive a LDAR flash and uncertainties associated with the calculation of the exact time of flash occurrence. It is noteworthy the narrow range of time lags (Figure 6c) associated with STARNET-NLDN matched flashes. The mean time lag is 0.34 milliseconds, while the mode of the distribution is at 0 milliseconds. This implies that STARNET and NLDN measures related lightning events.

Table 4 shows the percentage of matched flashes in respect to each system assuming ±250 and ±100 milliseconds timing window for LDAR-STARNET/NLDN matches and STARNET-NLDN matches, respectively. The LDAR flashes observed by NLDN and

STARNET systems are about 10% and 13%, respectively. These results show that higher timing windows are required to capture the entire lightning event, assuming that LDAR measures total lightning with DE above 90%. Consequently, these matches may not represent any measure of relative DE among the various instruments. At the present moment, CG and IC detection efficiency for LDAR system other than indirect comparisons has not been determined. Mazur et al. (1997) compared the LDAR system with the interferometric ONERA-3D (French experimental interferometric system) over Florida. They stated that each system measures a different radiation source: "*LDAR is associated with virgin breakdown process typical of slowly propagating negative leader; ONERA-3D is associated by the fast intermittent negative breakdown processes typical of dart leader and K changes as they traverse the previously ionized channels*". Therefore, LDAR comparisons with different frequency sensors are affected by differences in the properties of the radiating source. On the other hand, Boccippio et al. (2001b) compared LDAR with LIS to retrieve bulk flash detection efficiency values, assuming that LIS measures the "*true total lightning*", and used NLDN to retrieve location errors and its correlation. These results suggest that detection efficiency evaluation from different lightning sensors should be based on bulk relationships using larger time and space windows.

The matching observed between NLDN (~30%) and STARNET (40%) exhibits a better match among these systems than with LDAR. This reinforces that both systems tend to measure the same radiation source of a lightning event. Nevertheless, the two systems have different bandwidth frequencies and lightning identification schemes (i.e., NLDN uses the first 1-5 μsec of return stroke while STARNET computes the correlogram of electrical pulse shape using 13.1 msec time window). Consequently, the 60% mismatch between the two systems could be attributed to these differences, if assumed that both measure only CG.

The above results show lower frequency of match ups among the three systems. Consequently, we analyze the dependency of LDAR flashes as function of the matched NLDN and STARNET flashes. Figures 7a and 7b show scatter plots of the total lightning observed by LDAR in each 15-minute storm interval versus the matched STARNET and NLDN flashes, respectively. There is a tendency to find 4-6 LDAR flashes per STARNET flash, while for NLDN flash the ratio is 5-8 LDAR flashes. The observed variability is also an indication that varying storm systems and maturity levels have different IC:CG ratios, and therefore different detection levels for the three networks.

Next we present comparison of the total number of flashes observed by each system, in an attempt to indicate the proportionality among the different sensors. Figures 8a, 8b, and 8c show scatter plot comparisons (unconditional to matching) of total flashes observed in 15-minute storm intervals by each network. It is clear by figure 8b that LDAR-NLDN comparison does not show any evidence of relationship. Figure 8a shows also a large scatter between STARNET and LDAR, but a trend for relationship is observed. From Figure 8c it is evident a relationship between NLDN and STARNET and a tendency that STARNET observes more flashes than NLDN. This tendency can be interpreted as: (1) NLDN DE is lower than STARNET over Florida; and (2) STARNET measures additional lightning discharges associated with IC lightning.

In summary the above results showed that both NLDN and STARNET systems may measure IC flashes. It is also argued that evaluation of IC detection efficiency for either network on the basis of LDAR using a constrained time window matches is not adequate to obtain a reliable IC-DE. Furthermore, it was shown that all three systems measure lightning that oftentimes is not observed by the other two systems. For example, Figures 9 and 10 show the

spatial distribution and a time series of total flashes observed for a storm over Florida on February 22nd, 1998 by all three networks. Figure 9 (LDAR-left, STARNET-center, and NLDN-right panel) show that all systems delineated properly the thunderstorm. The LDAR system has larger spatial distribution, which indicates presence of more IC flashes. The time series of 10-second flash accumulations for the three networks (Figure 10) show both coincident and missed measurements among them. During 20:03 and 20:51 UTC there was no measurements of LDAR. We believe that the system did not work during that period even though the original raw data show continuous measurements with no indication of interruption. It is clear that on longer time interval accumulations we can find better matching between the different systems, while at finer scales this is not easy to obtain. Figure 11 shows time series for the same event but for 1-second flash accumulation between 21:30 and 21:45 UTC. This figure exemplifies where you can find several LDAR measurements not associated with STARNET and/or NLDN matches and vice versa. During the whole 15-minute period there is no LDAR flash matched with STARNET and NLDN, except at 21:34'43'' where there is only one match with STARNET. There are two NLDN observed flashes (21:37'33'' and 21:38'56'') and one STARNET flash (21:37'33'') not observed by LDAR. These results reinforce the argument that instead of trying to find coincident measurements in time and space it would be better to work on bulk estimates at larger space and time windows. In this concept, different lightning sensors could be compared to obtain some meaningful detection efficiency estimates.

The results presented herein reveal that an inter-comparison among the different instruments is affected by the assumptions applied. Each sensor measures lightning at different frequencies, which corresponds to different stages of the stroke. Therefore a direct evaluation of detection efficiency is not easy to be retrieved under the presented conditions. Consequently, in

section 4.2 we investigate a methodology that computes bulk IC-DE and CG-DE values for STARNET using combination of LDAR and NLDN as reference.

4.2 STARNET IC and CG DE over Florida: LDAR comparison

This section investigates STARNET's CG and IC detection efficiency using combination of LDAR and NLDN lightning information. The assumption is made that LDAR measures total lightning, namely, both CG and IC, with a detection efficiency of 100%. Furthermore, it is well accepted that NLDN measures mainly CG return strokes with high detection efficiency (~90%). Consequently, it is assumed in this analysis an NLDN flash is associated with CG lightning. The methodology proceeds as following. In the 301 selected storm cases presented in the previous section we calculated the number of cases where:

(1) There is corresponding LDAR, NLDN, and STARNET flashes, which are the STARNET CG catches ($N_{CG\text{-}Matched}$);
(2) There is LDAR and NLDN flash but no STARNET measurement, which are STARNET CG misses ($N_{CG\text{-}Missed}$);
(3) There is LDAR and STARNET flash but no NLDN, which are STARNET IC catches ($N_{IC\text{-}Matched}$);
(4) There is LDAR flash but no corresponding NLDN and STARNET measurement, which are STARNET IC misses ($N_{IC\text{-}Missed}$).

Subsequently, we define the cloud-to-ground (DE_{CG}) and intra-cloud (DE_{IC}) detection efficiency bulk statistics for STARNET as:

$$DE_{CG} = \frac{N_{CG-Matched}}{N_{CG-Matched} + N_{CG-Missed}} \quad (3)$$

$$DE_{IC} = \frac{N_{IC-Matched}}{N_{IC-Matched} + N_{IC-Missed}} \quad (4)$$

As already presented in section 4, small timing window matching constrains are not able to capture the entire lightning event in all three systems. Thomas et al. (2000) compared 3-D lightning measurements similar to LDAR system with LIS and NLDN over a storm event and found time differences ranging from 100 milliseconds up to 2 seconds for all three systems to observe the same lightning event. Consequently, here we evaluate the DE for several time intervals ranging from 250 milliseconds up to 2 seconds. Table 5 shows both CG and IC STARNET DE values computed from equations (3) and (4) based on the entire data set (301 storms) for daytime and nighttime conditions. Furthermore, the third column of Table 5 shows the CG-DE values assuming a 90% DE for NLDN as has been evaluated by Cummins et al. (1998).

These results show an overall STARNET CG DE ranging from 64% to 78% over Florida. During daytime conditions the STARNET CG-DE varies from 68% to 78%, while during nighttime it ranges from about 50% to 67%. These values are consistent with the CG-DE efficiency estimates of Section 3 that were independently evaluated based on STARNET-NLDN data comparisons. Furthermore, this analysis indicates IC inflation in STARNET measurements.

The overall IC DE of STARNET computed herein ranges from about 7% to 20%, while for daytime and nighttime conditions the STARNET IC-DE ranges from about 5% to 9% and 9% to 30%, respectively. The STARNET IC inflation presented in this analysis greatly explains the anomalous CG-DE efficiency retrieved in the East Coast of US for daytime conditions (see Figures 2 and 3). For nighttime conditions, we also observe similar CG-DE decay but with an increase of IC. This may be an effect of weak lightning sources that can travel larger distances during nighttime without been heavily attenuated.

The results presented herein offer strong evidence that VLF systems measure some IC lightning and provided quantification of its detection efficiency. Investigations of sferics waveform measured by those systems in the framework of the analyses presented herein could enable us to better characterize the sferics waveform associated with CG and IC lightning. Unfortunately the sferics waveform information is not available at the present data. Future systems, such as a sferic network being implemented in Europe by the National Observatory of Athens, can allow investigation of the separation of CG and IC lightning measurements through a better characterization of the sferics waveforms.

5. Bulk IC:CG ratios

According to the results presented in the previous sections, bulk ratios are suited to express the fraction of IC. This section computes the bulk IC:CG ratios over the continental US and the LDAR domain in Florida.

5.1 Continental US

The previous section showed that STARNET detects larger number of events than NLDN, which is widely accepted to measure CG lightning. Therefore, assuming that the excess of lightning flashes are IC flashes it is straightforward to retrieve the ratio of IC:CG from STARNET-NLDN data. This same assumption was made by Boccippio et al. (2001c) for computing the IC:CG ratios over the continental US using OTD and NLDN measurements.

In order to compute these ratios, we apply the detection efficiency relationships obtained in section (3), and accumulate the number of STARNET sferics and NLDN flashes (multiplied by the number of strokes observed in each flash and its correspondent DE) in 2 degrees longitudinal zones and 15-minute time intervals over the US. Thus the IC:CG ratio is defined as:

$$IC{:}CG = \frac{N_{sferics} - N_{NLDN}}{N_{NLDN}} \qquad (5)$$

where N_{NLDN} is the total number of CG flashes measured by NLDN multiplied by the number of strokes observed in each flash, and $N_{sferics}$ is the total number of sferics. The ratios (equation 5) evaluated for each 15-minute intervals are averaged to form hourly ratio values, which is expected to smooth some of the storm related IC:CG variability.

The evaluated IC:CG ratio values are presented in Figure 12 as blue asterisks. It is noted that there are some regions with low IC detection (i.e., below one). Nevertheless, most of the values are above one, which indicates higher IC detection. This figure also shows some strong deviations of IC:CG ratios from the mean at longitude ranges of 125W, 103-100W, and 80-75W.

This indicate that there is no unique value for IC:CG ratios, and climatic regions play an important role on the determination of this ratio.

We compare these results to the ones obtained by Boccippio et al. (2001c), and seem to be in some agreement. Boccippio et al. (2001c) computed climatological IC:CG ratios over the US based on 4 years of coincident measurements of OTD and NLDN. The mean, maximum, and minimum values of their IC:CG ratios as a function of longitude are shown in Figure 12 for reference. Note that the same peaks of IC:CG ratio values observed along the US in Figure 12 were also observed by Boccippio et al. (2001c).

5.2 Cape Canaveral: LDAR domain

In the previous section IC:CG ratios were computed for the whole continental US. These values can be further investigated by inspecting their variability over Florida. In this region, we can use LDAR measurements as a reference. A methodology is described for obtaining the IC:CG ratios based on results presented in previous sections.

The separation of IC and CG flashes for LDAR follows the definition presented in Section 4.2. Namely, an LDAR flash that has no correspondent NLDN flash within 2 seconds time window is considered CG, otherwise, it is an IC lightning. For STARNET and NLDN comparisons, it is assumed that NLDN measures only CG and the STARNET flashes missed by NLDN are considered as IC (see equation 5). The ratios are computed considering accumulations in 15-minute time intervals for each storm inside the 100 km range of LDAR central stations.

Figure 13 shows the IC:CG bulk ratio distributions for STARNET:NLDN (red) and LDAR (blue) data based evaluations. The STARNET:NLDN based IC:CG ratios show larger range of values than what was presented in Figure 12. In Figure 12, the ratios ranged from 0-4, while in Figure 13 these values represent just about 55% of the observed sample, which is due to the high variability of IC:CG at higher temporal distribution, since it is computed at 15 minutes storm intervals. The ratios derived by LDAR data are also consistently within the STARNET:NLDN range and show comparable distribution. However, LDAR tends to show higher IC:CG ratio values, which is expected from a system that measures total lightning with DE above 90%. These results indicate that the IC:CG ratio is quite variable and its value range depends strongly on storm maturity. The IC:CG ratios below one represent just less than 10% of the sample for both LDAR and STARNET:NLDN. Those values may indicate that: (1) STARNET is not measuring proportionally the corresponding IC flashes; (2) weak IC flashes are not measured by both STARNET and LDAR networks, and/or (3) LDAR might suffer block outs due to very high flash rates.

6. Conclusions

This paper described a methodology for retrieving empirically the CG detection efficiency of STARNET measurements relative to NLDN. Secondly, it investigated the detection efficiency of IC measurements by systems known to be dominated by CG measurements (i.e., NLDN and STARNET) using LDAR system measurements as a reference. Thirdly, bulk IC and CG detection efficiency statistics of STARNET were computed independently using as reference combination of LDAR and NLDN system measurements.

Finally, the paper presented evaluation of bulk IC:CG ratio values observed based on different lightning networks over the continental US and Florida.

Evaluation of the STARNET CG lightning measurements showed exponential range dependence, while daytime and nighttime CG lightning DE did not show notable differences, which indicates that STARNET sferics location algorithm properly accounts for the time variations of the VLF wave propagation in the earth-ionosphere wave-guide. Over the East Coast where STARNET's receivers are aligned the CG detection efficiency is 100%, while it drops exponentially to about 20% along the West Coast for both day and night hours.

As reported by Mazur et al. 1997, the comparison between two systems that measure lightning is subject to the properties, or radiation sources, of the lightning event emitted in the sensors frequency. The comparison between LDAR, NLDN and STARNET networks was limited by the sensors ability to measure a determined stage of the radiation source emitted by lightning at their particular bandwidth of operation. Therefore, evaluation of the STARNET, or NLDN, IC detection efficiency by a third system (LDAR) using timing window constrains for correspondent matches is complicated and likely biased. Consequently, STARNET IC and CG DE was determined statistically assuming that LDAR measures total lightning and NLDN only CG lightning with DE above 90% for both systems. The combination of those two measurements was used to separate the two types of lightning observed by STARNET. Results from this analysis showed for a first time substantial evidence of IC measurements by a VLF system. Additionally, the study provided quantification of the IC DE for the current STARNET VLF system. The overall CG and IC DE was shown to vary from about 57% to 70% and 7% to 20%, respectively, depending on the time window selection. Furthermore, detection efficiency was shown to have day and night dependence.

Finally, this study evaluated the bulk IC:CG ratios based on a larger time and space window. The STARNET and NLDN analysis showed a range of 0-4 in bulk IC:CG ratio values over the continental US, which agrees with previous calculations by Boccippio et al. (2001c), and Pierce (1970). In a finer space and time scale over Florida-US, the bulk IC:CG ratios based on LDAR and STARNET:NLDN comparisons showed similar distributions between the two methods, but higher range of values than what was evaluated over the Continental US. This is a consequence of storm variability and storm maturity that reflects the different stages of the cloud convection activity.

Acknowledgements: We acknowledge and appreciate useful discussions and input from Dr. Steve Goodman of NASA/MSFC, and Dr. Earle Williams of MIT. This research used sferics data from the Sferics Timing and Ranging Network (STARNET) implemented by Resolution Displays, Inc., under funding by NASA Small Business Innovative Research grant (NAS5-32825). The authors are thankful to Mr. Stan Kriz from RDI for providing insightful information of the STARNET system's design and operation. This study was supported by NASA New Investigator Program award under Grant NAG5-8636. The first author was also supported by the Conselho Nacional de Desenvolvimento Científico e Tecnológico (CNPq) under grant 260133/93.0 of the Brazilian government.

7. References

Boccippio, D.J., S. Heckman, and S,J. Goodman, 2001a: A diagnostic analysis of the Kennedy Space Center LDAR network: I Data characteristics. J. Geophys. Res., 106, D5, 4769-4786

Boccippio, D.J., S. Heckman, and S,J. Goodman, 2001b: A diagnostic analysis of the Kennedy Space Center LDAR network: II Cross-sensor studies. J. Geophys. Res., 106, D5, 4787-4796.

Boccippio, D.J., K.L. Cummins, H.J. Christian, and S.J. Goodman, 2001c: Combined satellite and surface-based estimation of the intracloud/cloud-to-ground lightning ratio over the continental United States. Mon. Wea. Rev., 129, 1, 108-122.

Challinor, R.A., 1967: The phase velocity and attenuation of audio-frequency electromagnetic waves from simultaneous observations of atmospherics at two spaced stations, J. Atmos. Terr. Phys., 299, 803-810.

Chapman, F.W. and R.C.V. Macario, 1956: Propagation of audio frequency radio waves to great distances, Nature, 177, 930.

Christian, H.J., K.T. Driscoll, S.J. Goodman, R.J. Blakeslee, D.A. Mach, and D.E. Buechler, 1996: The Optical Transient Detector (OTD), Proceedings of the 10th Inter. Conf. on Atmos. Electricity, Osaka, Japan, 368-371.

Christian, H.J., R.J. Blakeslee, S.J. Goodman, D.A. Mach, M.F. Stewart, D.E. Buechler, W.J. Koshak, J.M. Hall, W.L. Boeck, K.T. Driscoll, and D.J. Boccippio, 1999: The Lightning Imaging Sensor. Proceedings of the 11th Int. Conf. on Atmos. Electricity, Guntersville, Alabama, 746-749.

Cramer, J.A. and K.K. Cummins, 1999: Long-Range and Trans-Oceanic Lightning detection, 11th International Conf. Atmos. Electricity, 376-379.

Cummins, K.L., M. Murphy, E. Bardo, W. Hiscox, R. Pyle, and A. Pifer, 1998a: A combined TOA/MDF technology upgrade of the U.S. National Lightning Detection Network, J. Geophys. Res., 103, 9035-9044.

Cummins, K.L., E.P. Krider, M.D. Malone, 1998b: The U/S national lightning detection network and applications of cloud-to-ground lightning data by electric power utilities, IEEE Trans. Elec. Comp., 40, 465-480.

Horner, F., 1964: Radio noise from thunderstorms, Advances in Radio Research, Ed. J.A. Saxton, vol. 2, 122-204.

Idone, V.P., D.A. Davis, P.K. Moore, Y. Wang, R.W. Henderson, M. Ries, and P.F. Jamason, 1998, Performance evaluation of the U.S. National Lightning Detection Network in eastern New York, 1: Detection efficiency, J. Geophys. Res. 103, num. D8, 9045-9055.

Koshak, W.J. and R.J. Solakiewicz, 1996: On the retrieval of lightning radio sources from time-of-arrival data, J. GEOPHYS. RES-ATMOS., 101 (D21), 26631-26639.

Krider, E.P., R.C. Noggle, M.A. Uman, 1976: A gated wideband magnetic direction-finder for lightning return strokes, J. Appl. Meteor., 15, 301-306.

Lee, A.C.L., 1986a: An experimental study of the remote location of lightning flashes using a VLF arrival time difference technique, Quart. J. R. Met. Soc., 112, 203-229.

Lee, A.C.L., 1986b: An operational system for the remote location of lightning flashes using a VLF arrival time difference technique, J. Atmos. and Ocean. Tech., 3, 630-642.

Lee, A.C.L., 1989: The limiting accuracy of long wavelength lightning flash location, J. Atmos. and Ocean. Tech., 6, 43-49.

Lennon, C. and L. Maier, 1991: Lightning mapping system, Proc. Int. Aerospace and Ground Conf. On Lightning and Static Electricity, Cocoa Beach, FL, NASA Conf. Pub. 3106, II, 89.1-89.10.

Lewis, E.A., R.B. Harvey, and J.E. Rasmussen, 1960: Hyperbolic direction finding with sferics of transatlantic origin, J. Geophys. Res., 65, 1879-1905.

Malan, D.J., 1963: Physics of Lightning, The English Universities Press, London, 176 pp.

Mazur, V. E. Williams, R. Boldi, L. Maier, and D.E. Proctor, 1997: Initial comparison of lightning mapping with operation Time-of-Arrival and interferometric systems. J. Geophys. Res., 102, D10, 11071-11085.

Morales, C. A., E. N. Anagnostou, J. A. Weinman, 2001: Continuous Long-Range Thunderstorm Monitoring by VLF Receiver Network, Part I: Location Error Analysis, Submitted to J. Atmos. Ocean Tech.

Orville, R.E., 1991: Lightning ground flash density in the contiguous United States – 1989, Mon. Weather Rev., 119, 573-577.

Pierce, E.T., 1970: Latitudinal variation of lightning parameters, J. Appl. Met., 9, 194-195.

Pierce, E.T., 1977: Atmospherics and radio noise, in

Lightning, vol. 1, Physics of Lightning, R.H. Golde, 351-384.

Proctor, D.E., 1971: A hyperbolic system for obtaining VHF radio pictures of lightning, J. Geophys. Res., 76, 1478-1489.

Saxton, A.A., 1964: Advances in Radio Research, Academic Press.

Taylor, W.L., 1960a: Daytime attenuation rates in the V.L.F. band using atmospherics, J. Res. Nat. Bur. Stand., 64D(Radio Prop.), 349.

Taylor, W.L., 1960b: V.L.F. attenuation for east-west and west-east daytime propagation using atmospherics, J. Geophys. Res., 65, 1933.

Taylor, W.L., and L.J. Lange, 1958: Some characteristics of v.l.f. propagation using atmospherics waveforms, Proc. Second Conference on Atmos. Electricity, p. 609, Pergamon Press, London.

Thomas, R., P. Krehbiel, W. Rison, T. Hamlin, D. Boccippio, S. Goodman, and H. Christian, "Comparison of ground-based 3-dimensional lightning mapping observations with satellite-based LIS observations in Oklahoma", Geophys.Res. Lett., 27, 1703-1706, 2000.

Wacker, R., and R. Orville, 1999a: Changes in measured lightning flash count and return stroke peak current after the 1994 U.S. National Lightning Detection Network upgrade: I. Observations. J. Geophys. Res. 104, 2151-2157.

Wacker, R., and R. Orville, 1999b: Changes in measured lightning flash count and return stroke peak current after the 1994 U.S. National Lightning Detection Network upgrade: II. Theory. J. Geophys. Res. 104, 2159-2162.

Wait, J.R, 1970: Electromagnetic waves in stratified media, Pergamon Press.

Table 1. Attenuation coefficient values used for different propagation directions and land/sea surfaces.

Propagation Time	Direction	Land (dB/Mm)	Sea (dB/Mm)
Daytime	East-West	4.5	3.6
	West-East	3.0	2.5

Table 2: Total number of matched Sferics/NLDN pairs for different space and timing windows over the continental US. A total number of 871,450 CG flashes were observed by NLDN and 1,095,928 sferics by STARNET in this period.

$\varepsilon_{t(max)}$ / $\varepsilon_{t(max)}$	10 km	50 km	100 km
20 ms	172,544	405,721	471,804
40 ms	183,826	430,930	503,830
60 ms	200,494	469,156	551,231
100 ms	236,288	552,856	654,238
150 ms	274,719	649,092	796,622
200 ms	304,043	720,767	864,181

Table 3: Least squares fits of sferics cloud-to-ground detection efficiency versus longitude westward from the East Coast network and time of the day over the continental US.

Cloud to Ground Detection Efficiency (100 ms and 50 km space-time window)	Range: 70-130 W
Daytime **(08-16 Local time)**	exp{7.40298 + 0.036726*λ}
Twilight Day **(05-07 Local Time)**	exp{7.05156 + 0.034000*λ}
Nighttime **(00-04 and 20-23 LT)**	exp{6.44210 + 0.027800*λ}
Twilight Night **(17-19 Local Time)**	exp{7.09480 + 0.034700*λ}

Table 4. Frequency (%) of matches in respect to each network system and total number of flashes observed by LDAR, NLDN and STARNET networks.

Network	LDAR	NLDN	STARNET	Total
LDAR	100.00 %	23.23 %	22.07 %	16,349
NLDN	10.44 %	100.00 %	40.30 %	7,347
STARNET	13.04 %	30.66 %	100.00 %	9,656

Table 5: Overall, day and nighttime STARNET CG and IC DE efficiency for different timing matching intervals and all 301 storm cases.

	Overall			**Daytime**		**Nighttime**	
ΔT(msec)	CG	CG x DE_{NLDN}	IC	CG	IC	CG	IC
250	57.97	64.41	7.77	68.08	4.91	49.72	9.93
500	61.30	68.11	11.21	72.46	6.12	54.14	15.18
1000	64.35	71.50	15.38	74.98	7.04	58.84	22.36
2000	70.48	78.32	19.77	78.34	9.08	66.90	29.84

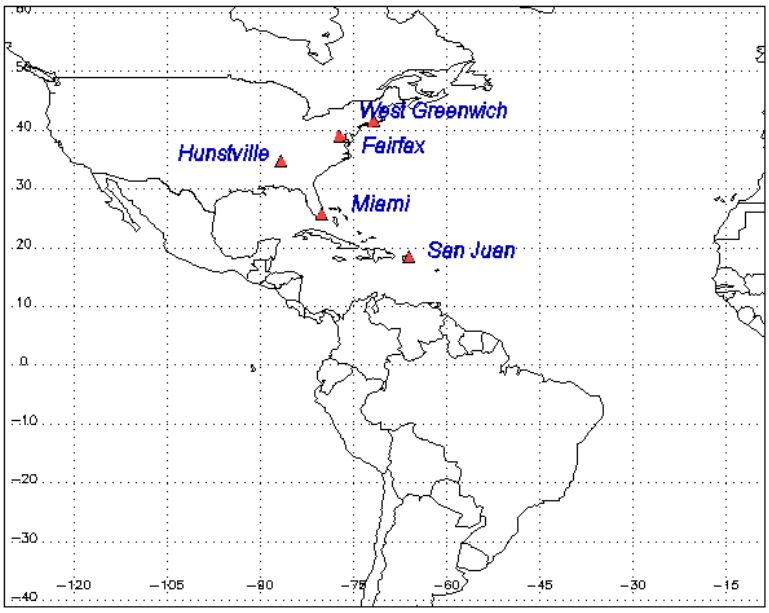

Figure 1. Location of STARNET radio receivers.

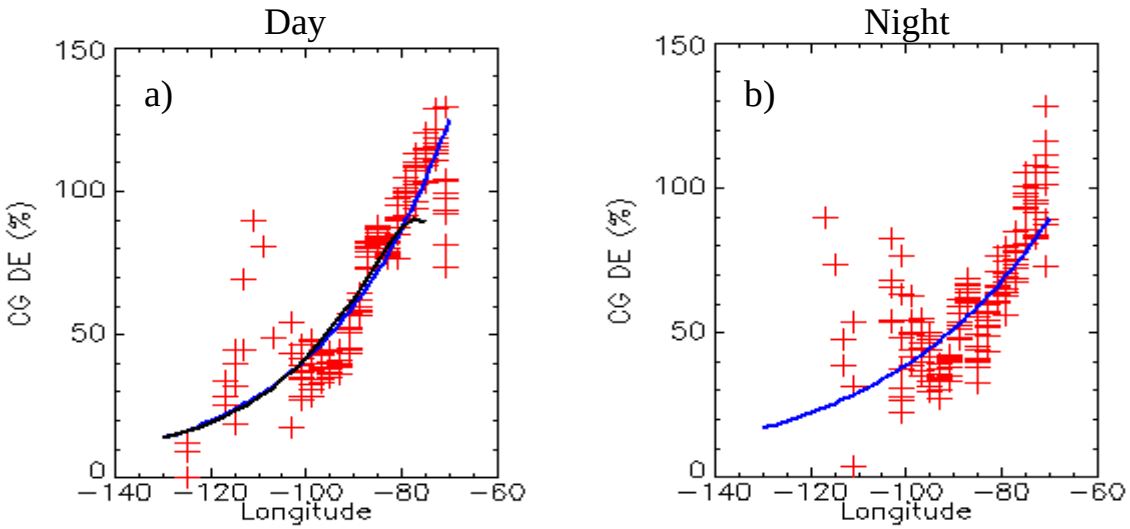

Figure 2: Sferics cloud-to-ground detection efficiency during the daytime (a) and nighttime (b) period for a timing window of 100 ms, and 50 km space window. The blue line represents the best fit of DE determined as a function of longitude. The black line is the DE determined from equation (1).

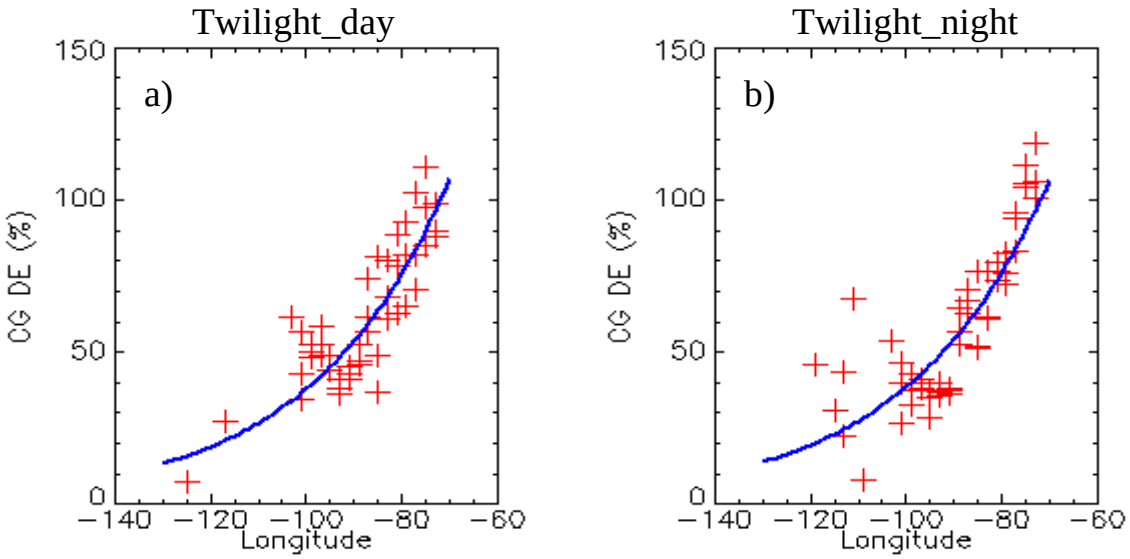

Figure 3: The same as in Figure 3, but during day and night twilight-time period.

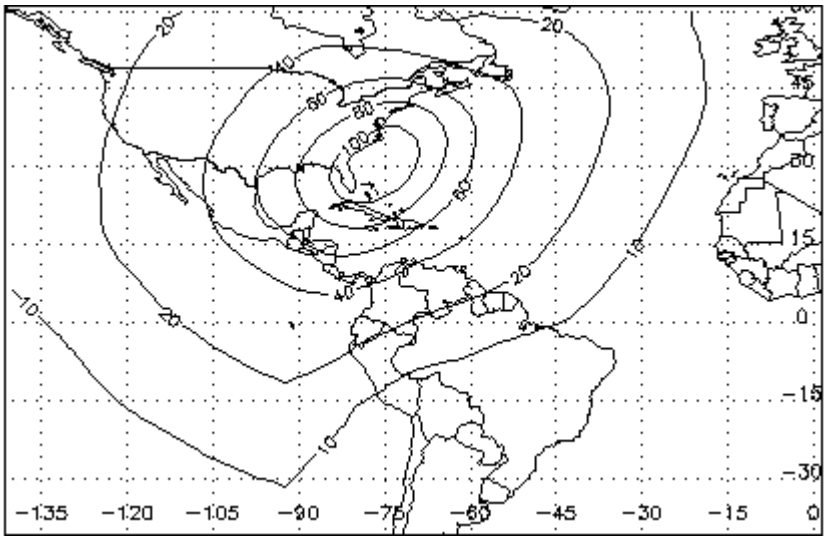

Figure 4. Daytime STARNET's CG DE spatial distribution evaluated using the theoretical signal strength model adjusted by the experimentally derived CG DE values.

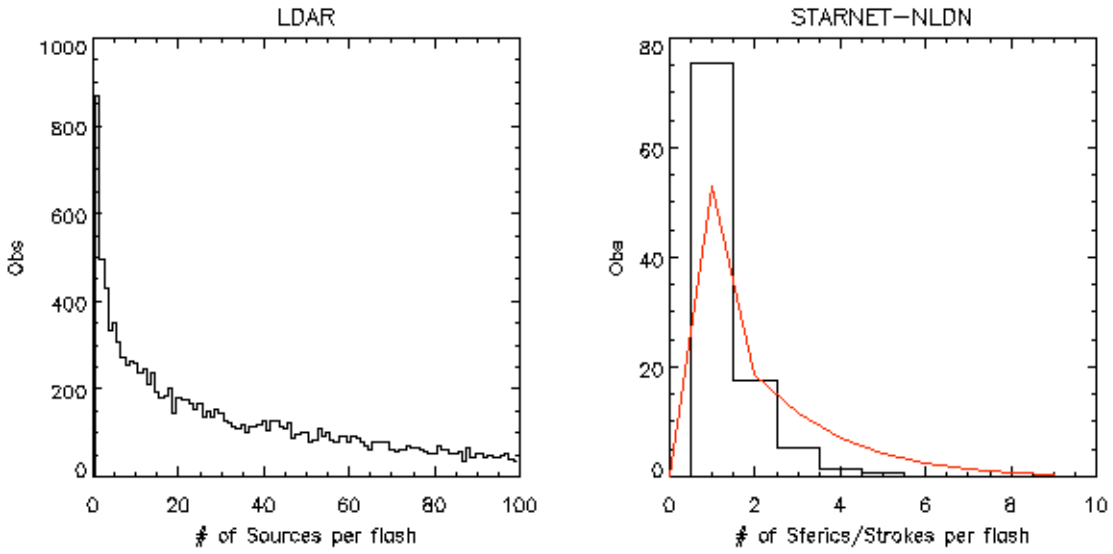

Figure 5. (a) Left panel, histogram of LDAR source number per flash; (b) right panel, histogram of number of STARNET (black) sferics events and NLDN (red) strokes per flash. These results are based on storms observed within 100 km range from the LDAR central station.

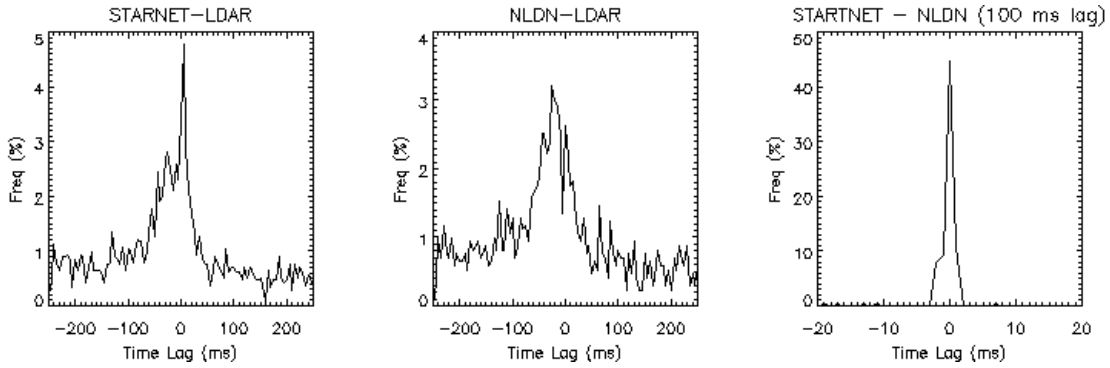

Figure 6. Time lag distribution of LDAR vs. STARNET matches (left panel), NLDN vs. LDAR matches (center panel), and STARNET vs. NLDN matches (right panel). Negative time lags represent time delay with respect to LDAR (left two panels), or STARNET to NLDN (right most panel), while positive is the contrary.

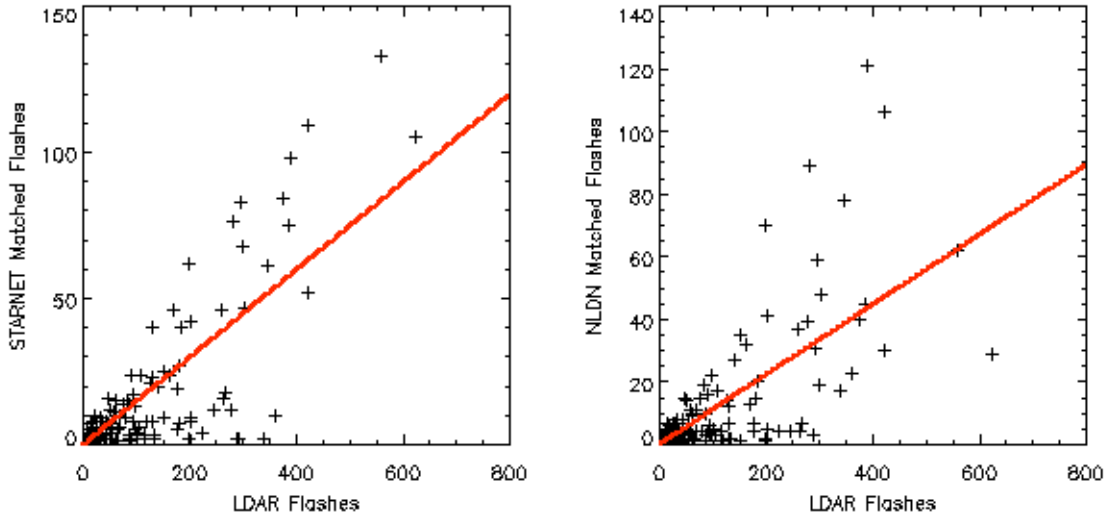

Figure 7. LDAR total lightning flashes versus total STARNET (left panel) and NLDN (right panel) matched flashes for each of the 301 selected 15-minute storm cases. The red lines represent the least-square fit of the above data set.

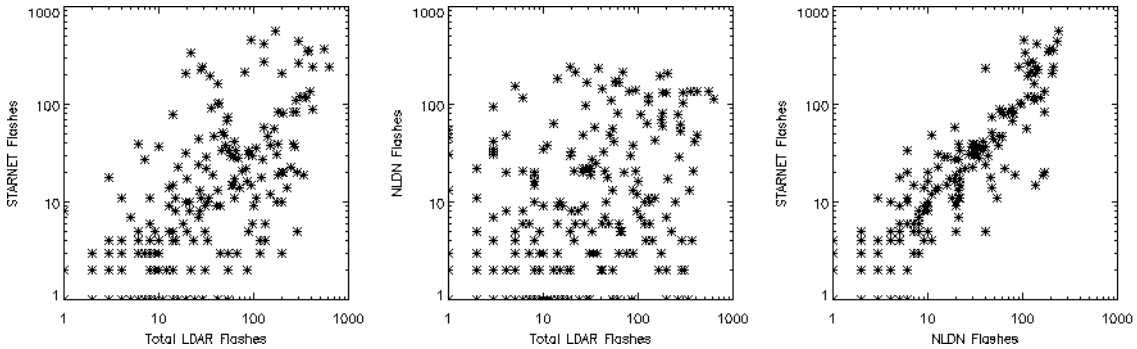

Figure 8. LDAR versus STARNET (left panel) and NLDN (middle panel) total flashes within the 15-minute storm intervals; Right panel, NLDN versus STARNET total flashes.

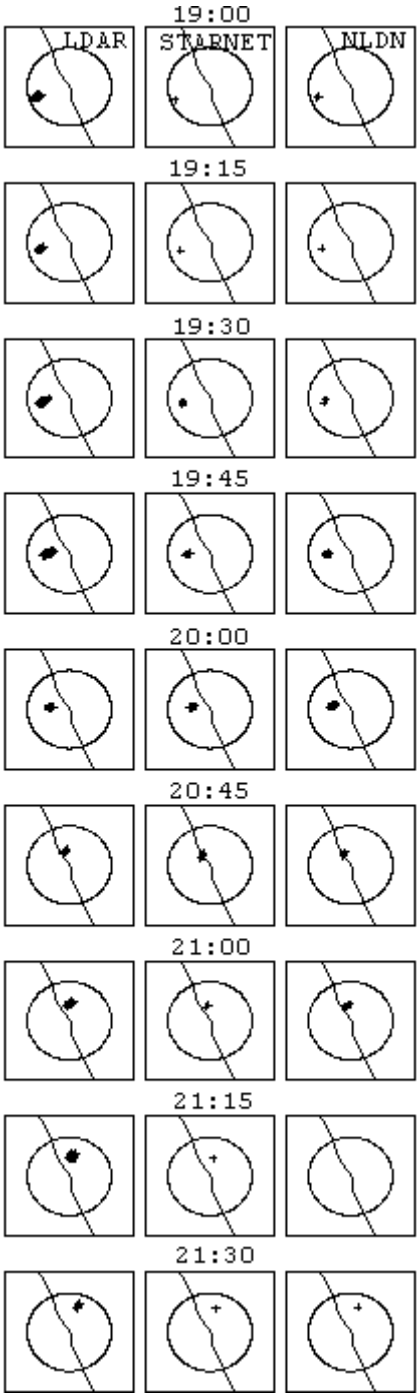

Figure 9. Spatial distribution of observed LDAR (left), STARNET (center) and NLDN (right) flashes at 15-minute intervals. The circle radius is 100 km and the center is at LDAR central station.

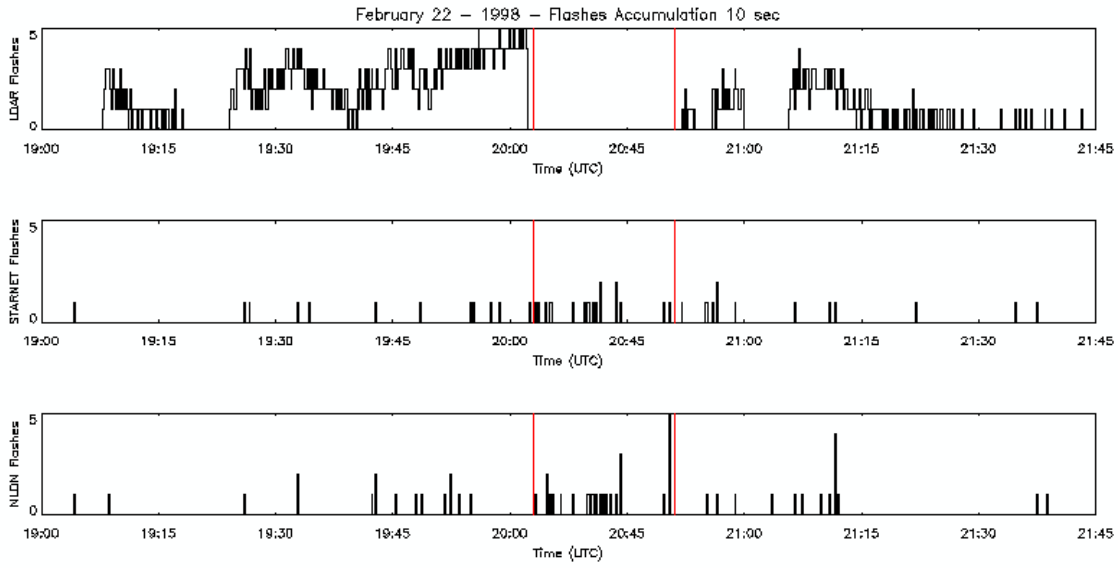

Figure 10. Time series of total flashes accumulated on 10-second intervals observed on February 22nd 1998 (19:00 UTC through 21:45 UTC) by LDAR (top), STARNET (center), and NLDN (bottom). Note that during 20:02-20:52 there were no available LDAR data (red bars) (The 20:45 UTC time also coincides with 20:15 UTC).

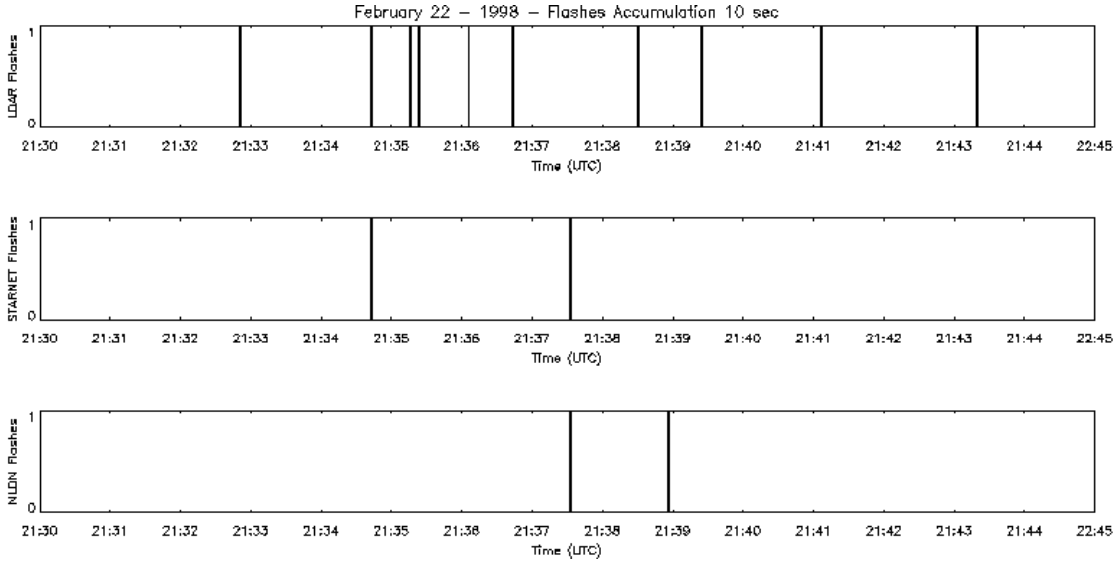

Figure 11. Time series of total flashes accumulated on 1-second intervals observed on February 22nd 1998 for LDAR (top), STARNET (center), and NLDN (bottom) from 21:30 UTC through 21:45 UTC.

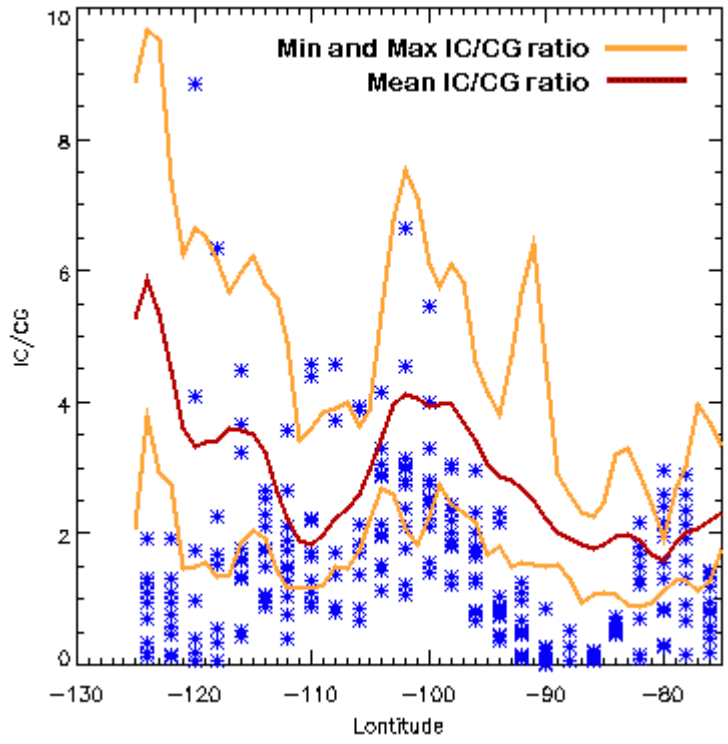

Figure 12: Mean IC:CG ratio values for hourly intervals over 2 degree longitude zones for the period of December, 1997 through February 1998 (blue asterisks). Red and yellow lines represent mean and maximum/minimum values of IC:CG OTD/NLDN ratios evaluated by Boccippio et al. (2001c).

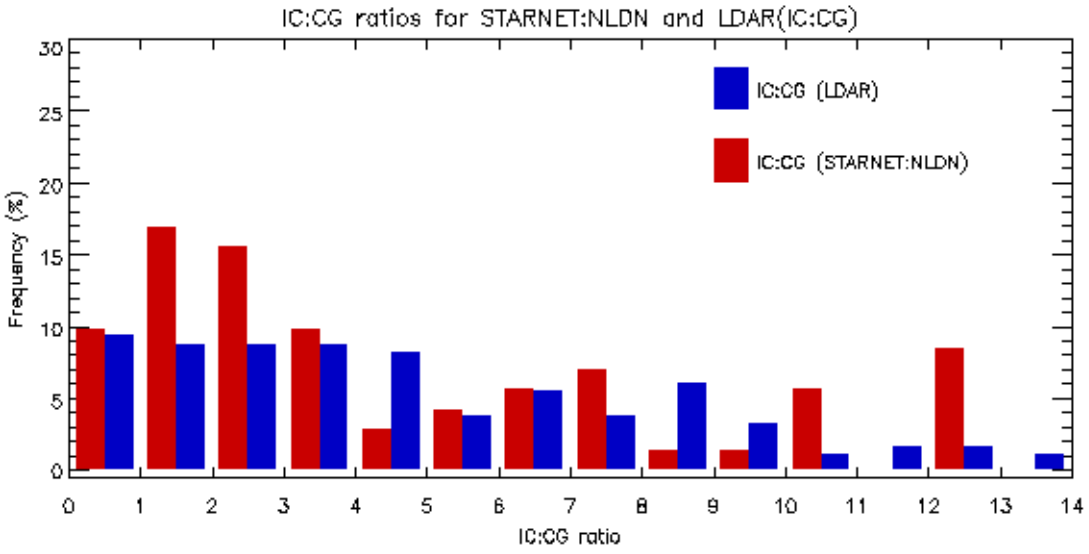

Figure 13. Histogram distribution of bulk IC:CG ratio values derived from STARNET:NLDN (red) and LDAR (blue) data for 301 storms with 15 minutes time interval.